

Cerebellar Neuropathology in Classical Scrapie

Subjects: Neurosciences

Contributor: Adolfo Toledano

Classical scrapie is a naturally transmissible spongiform neurodegenerative disease that originally affected sheep, goats and mouflons and that has been observed for several centuries. It is a “strange” disease that cannot be classified as a classical bacterial or viral infectious disease and does not follow the pathogenic patterns identified by infectious or neurodegenerative disease research.

Keywords: classical natural scrapie ; cerebellum ; Purkinje cells ; calbindin immunoreactivity ; calretinin immunoreactivity ; astrogliosis ; microgliosis ; spongiosis ; abnormal PrP deposits/deposition

1. Introduction

Scrapie is an infectious disease of sheep that has been documented since 1700 ^[1], and it has been assigned various names throughout Europe. Its existence was later verified in goats ^[2]. Its origins may lie in Merino sheep in Spain, and its existence has been known since the 16th century (“trembling sheep”, “Tembladera”). The name scrapie refers to the lumbar itching of infected animals.

Both classical scrapie and prion-like diseases induce neurodegeneration, with abundant neuropathological manifestations observable at the level of light and electron microscopy. Four important groups of alterations can be considered: (1) neuronal changes, (2) “spongiform” vesicular (or vacuolar) formations, (3) neuroglial alterations and (4) aberrant prion protein (PrP) deposits/deposition ^{[3][4][5][6][7][8][9]} (Figure 1).

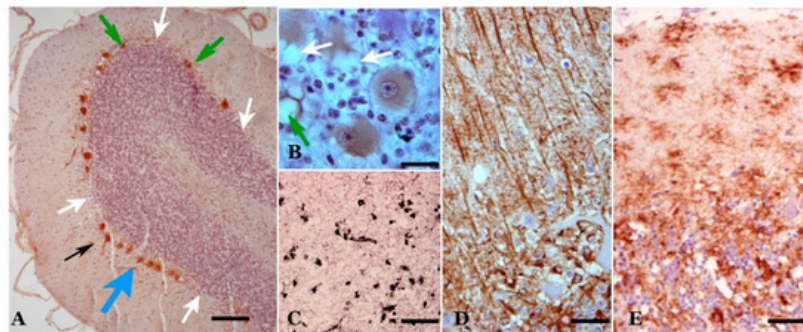


Figure 1. Main neuropathological alterations in classical scrapie. (A) Neuronal changes and loss. In these cerebellar folia, Purkinje neurons of different morphologies are observed: normal, hypertrophic (black arrow), atrophic (green arrows) and dystrophic (blue arrow). Likewise, areas exist where neurons have been lost (white arrows). Calbindin immunostaining plus hematoxylin contrast. (B) “Spongiform” (vacuolar) structures. Vesicles of different types are seen both in the neuropil (green arrow) and in the cytoplasm of neurons (white arrows). Calbindin immunostaining plus hematoxylin contrast. (C,D) Neuroglial reactivity. In (C), microgliosis is shown (proliferation of different types of microglia—rounded or branched). LN3 immunostaining plus Ni contrast. In (D), astrogliosis (hypertrophy, hyperplasia and increased number of gliofibrils) is shown. GFAP immunostaining plus hematoxylin contrast. (D) Abnormal prion protein (PrP) deposits/deposition. Various types of accumulations in the neuropil associated with cells, both in the form of dispersed or coalescent granulations and in a star-like shape. Abnormal PrP immunostaining plus hematoxylin contrast. (E) Abnormal PrP immunostaining plus hematoxylin contrast. (Bar: A = 125 μ m; B = 20 μ m; C = 125 μ m; D = 30 μ m; E = 35 μ m).

2. Neuropathologic Alterations of the Cerebellum in Classical Scrapie

2.1. Neuronal Alterations

We do not consider the decreases in cell density in the sheep breed that we have studied (*Rasa Aragonesa*) significant when faced with senile involution, especially in preclinical or clinical phases. However, the histochemical changes of many neurons that can be the basis of the dysfunctions of the cerebellar circuits were significant ^{[3][4][5]}. It is important to note

that the changes are different in the different cerebellar lobes and circumscribed areas in different lobes because they show important patterns (hyper- and hypo-reactivity of various markers and hypertrophy or atrophy of neurons) ([Figure 2](#), [Figure 3](#) and [Figure 4](#)). This could be more related to special “modules” or “functional circuits”, which are not yet well defined, within the apparent histological uniformity of the cerebellum. Moreover, individual responses of neurons in a specific subtype are always observed ([Figure 2](#), [Figure 3](#) and [Figure 4](#)). Ongoing investigations are attempting to differentiate the changes in different zebrine-positive or -negative strips and other possible functional zones, but have not yet yielded positive results, which have been observed in atypical scrapie.

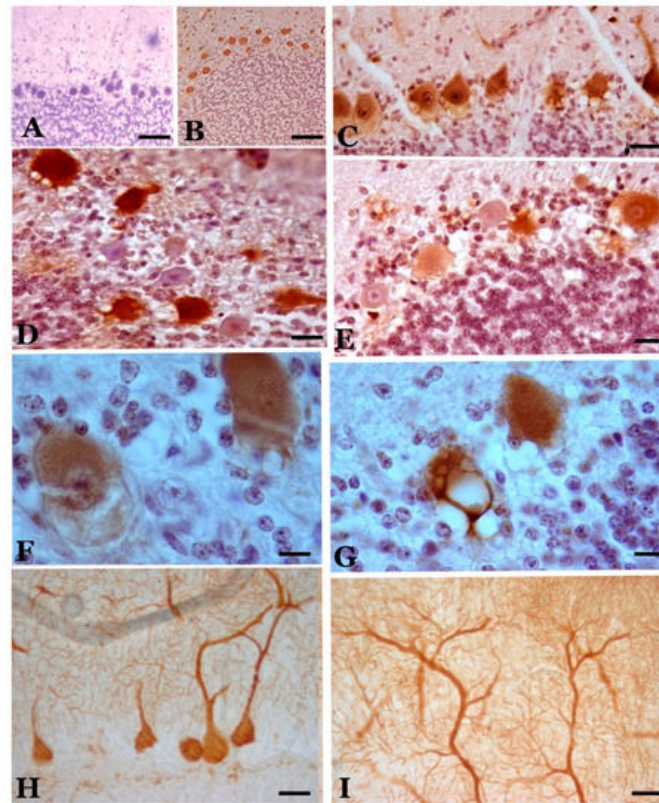


Figure 2. Calbindin-immunopositive Purkinje cells in control (**A**) and scrapie-affected sheep (**B–I**). (**B**) Cells of normal appearance in a case of preclinical scrapie, with a similar pattern to the control cases. (**C**) Cells of different appearance (normal, hypertrophic, dystrophic with rarefaction of their cytoplasm) in a case of clinical scrapie. (**D,E**) Cells of very different immunoreactivity in two cases of terminal scrapie. (**F**) Cytoplasmic rarefaction of the basal cytoplasm in an immunopositive cell of clinical scrapie. (**G**) Intense vacuolization in a positive cell. (**H,I**) Hypertrophic/hyperreactive cells. In (**H**), the hypertrophy of the initial dendrites is shown, and in (**I**), the hypertrophy of the distal dendrites that reach the pia mater. (**A–F**), hematoxylin contrast; (**H,I**), without contrast. (Bar: A, B = 125 μ m; C–E = 25 μ m; F, G = 20 μ m; H, I = 30 μ m).

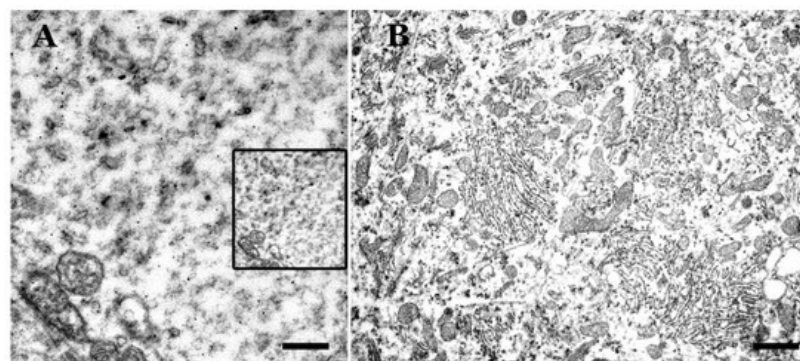


Figure 3. Electron microscopy images of the basal region of non-normal Purkinje neurons. Scrapie sheep in clinical phase. (**A**) Dystrophic cell with cytoplasmic rarefaction (dissolution/loss of subcellular organelles). Not defined debris are observed. Tubulo-vesicular formations appear (more notable in the upper left part of the image) as well as other electron-dense microvesicles. Insert: magnification similar to (**B**) for comparison. (**B**) Hypertrophic cell (diameter, 42 μ m) with a great abundance of subcellular organelles, although rough endoplasmic reticulum (RER) is more disorganized. Selected cytoplasmic regions are similar of those control neurons, but others resemble what is seen in dystrophic neurons (Bar: A = 0.5 μ m; B = 3 μ m).

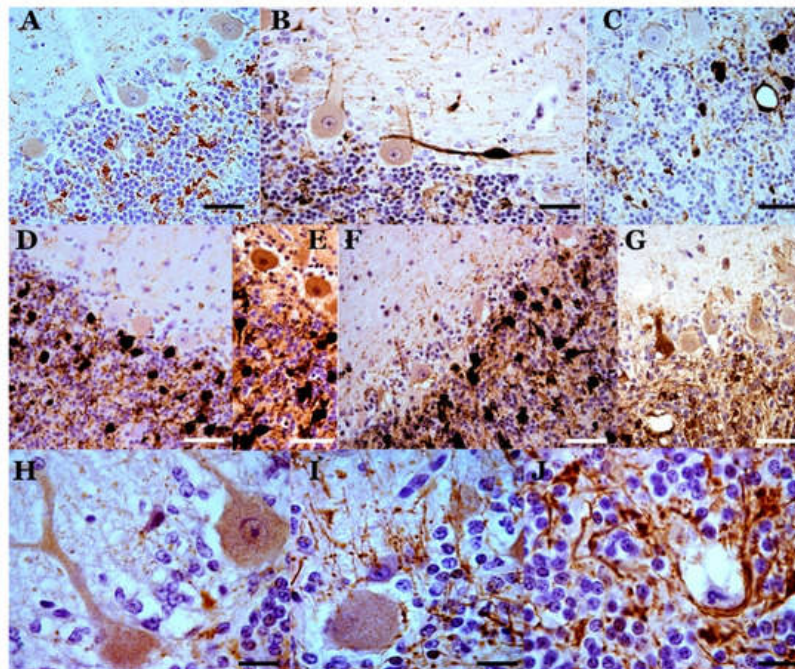


Figure 4. Calretinin-immunopositive cells in the cerebellar cortex of scrapie sheep (hematoxylin contrast). (A–C) Lobe VI (neocerebellum). In A, a slight reaction in Purkinje cells (PCs) and a greater intensity in some Golgi and brush cells of the granule cell layer as well as positivity in some parallel fibers are observed in a case of preclinical scrapie, a pattern similar to that shown by healthy controls. In (B), a case of clinical scrapie, the reaction pattern is maintained, although the intensity of the reaction is greater in some Purkinje neurons and cells of the granule cell layer (in the image, a Lugaro cell). In (C), a case of terminal scrapie, a very intense reaction is seen in hypertrophic Golgi cells of the granule cell layer (a vacuole is surrounded by its dendrites). The number of immunopositive Purkinje cells appears to decrease. (D–G) Lobe X (archicerebellum). In (D) and (E), a great diversity of reactions is observed in Purkinje cells (from negative to slightly positive in (D) to strongly positive in (E) as well as an intense reactivity in Golgi and brush cells of the granule cell layer. (The cell density of these cell types is 3–5 times higher than those observed in the neocerebellum). The reaction pattern is the same as that shown in control cases. In terminal cases (F), it seems to increase the reactivity in Purkinje cells (some of them are very hyperreactive) and decrease the intensity of the reaction in cells of the granule cell layer. (G) Detail of hyperreactive hypertrophic Purkinje cells in a case of clinical scrapie. (H) Hypertrophic/hyperreactive PCs in clinical phase. (I) Thin calretinin-positive varicose fibers that are prolongations of astrocytes of the granule cell layer to the molecular layer (“Weigert fibers”), observable only in clinical and terminal cases. (J) Detail of the elongation of monopolar dendrites and axons of brush cells that form loops in their path between grains and vesicles. Clinical scrapie case. (Bar: A = 40 μ m; B = 25 μ m; C–G = 40 μ m; H–J = 20 μ m).

2.2. Neuroglial Alterations

Astroglia: GFAP immunostaining in healthy (control) sheep showed intense immunoreactivity in Bergman fibers and astrocytes in the molecular, PC and granule cell layers (Figure 5) and deep internal nuclei. A similar general pattern of glial distribution has been observed in preclinical scrapie-affected sheep (Figure 5). Nevertheless, quantitative differences existed concerning immunolabeling in the granular layer close to PC as well as in the white matter, which increased the reactivity compared to the controls.

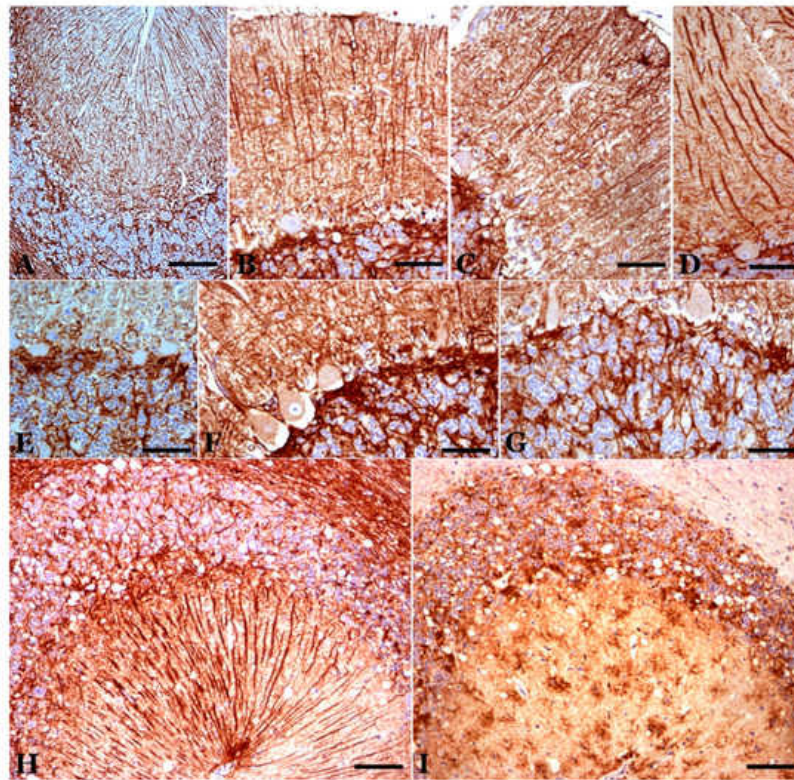


Figure 5. Astrogliosis in the cerebellar cortex of preclinical (A), clinical (B–F) and terminal (G) scrapie cases (GFAP immunostaining plus hematoxylin contrast). In the preclinical stage, the astroglial pattern is similar to that observed in controls. In the clinical stage, greater astrogliosis is observed, which can present different characteristics in different folia. In (B) and (C), there is hyperreactivity and hypertrophy in the astrocytes of the granular layer and in the Bergmann fibers of the molecular layer. In (D), great hypertrophy of these fibers is shown. (E) and (F) show greater astrogliosis in the basal area of the Purkinje layer. (G) Astrogliosis in a case of terminal scrapie. (H,I). Parallel GFAP-immunostained (H) and abnormal PrP-immunostained (I) sections, respectively. There is a coincidence of granular deposits of abnormal PrP deposits/deposition in the Purkinje layer and the granule cell layer, but the star-shaped deposits in the molecular layer do not correspond to GFAP-immunopositive stellate astrocytes in the molecular layer. (Bar: A = 50 μ m; B–E = 40 μ m; F,G = 25 μ m; H,I = 50 μ m).

Oligodendroglia: Very few papers have been devoted to the study of oligodendroglia (including pro-oligodendrocytes or NG2 cells) in scrapie. Additional work on NG2 cells will be included in another chapter of this Special Issue.

Microglia: Most studies have shown that microglial cells increase in all layers of the cerebellar cortex (Figure 1) and the central cerebellar nuclei, with a moderate increase in the preclinical phase a more intense one in the terminal phase. In the preclinical phase, only star-like microglial cells were observed in areas near some PCs. In the clinical and terminal phases, large areas of all layers of the cerebellar cortex and deep cerebellar nuclei presented an increase in reactive microglial cells, including stellate forms and round phagocytic-shaped cells.

2.3. Spongiform Alterations

In the middle part of the granule cell layer, near the PC layer or in several areas of the molecular layer, vacuole-like structures were observed in scrapie-affected sheep. When these vesicles were studied in CB-, CR- or GFAP-immunostained sections, some of them were surrounded by CR-immunopositive neuronal structures (fibers and very dystrophic large cells), Purkinje neurons and/or glial-like processes (in both mild and intense immunopositivity) (Figure 2, Figure 4 and Figure 5). Sometimes, areas with these vacuolar structures lying close together with more intense abnormal PrP-immunoreactive deposits were observed in parallel sections immunostained for the prion protein (Figure 5 and Figure 6).

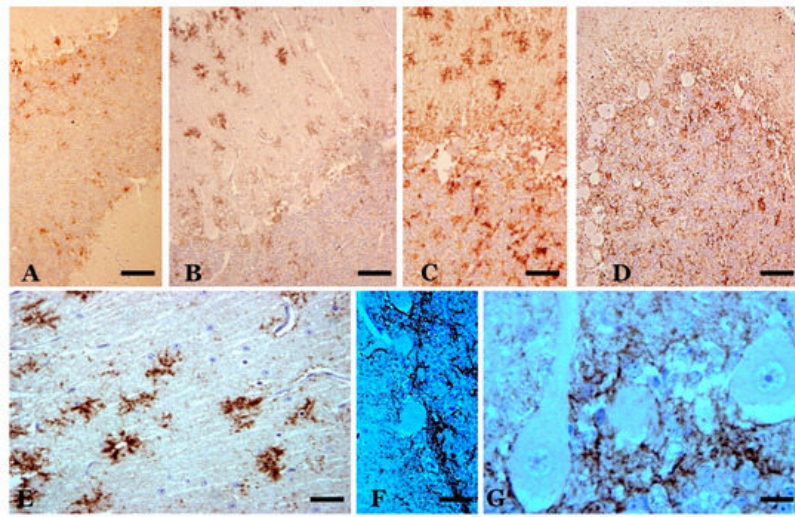


Figure 6. Abnormal PrP deposits/deposition (abnormal PrP immunoreaction—L42 1/500; Bio-Pharm, Darmstadt, Germany—plus hematoxylin contrast). (A) Deposits in a sheep in the preclinical phase of scrapie. Slight deposits are observed only in some folia in the layers of the cerebellar cortex. (B,C) Star-like deposits in the molecular layer (in B) and various types of deposits in all layers in two cases of sheep with infection in the clinical stage. (D) Diffuse granular deposits in all layers of a terminal-phase sheep case. Star-like deposits do not appear. (E–G) Details of prion deposits in clinical phase. In (E), star-like deposits are seen, which suggest association with non-GFAP-immunopositive astroglial cells. Hematoxylin-stained glial nuclei are seen in some of these deposits. In (F), a high degree of coalescence of the granular deposits is observed in the basal area of the Purkinje layer, similar to dense formations of astroglial processes in these areas (see Figure 4). In (G), a large accumulation of granular prion deposition is observed surrounding the areas of dystrophic Purkinje cells (with rarefied cytoplasm), but without the appearance of abnormal PrP immunoreaction in these cells. Abnormal PrP immunoreaction with hematoxylin contrast (in different concentrations). (Bar: A–D = 40 μ m; E = 10 μ m; F = 25 μ m; G = 10 μ m).

2.4. Deposits of Aberrant Prion Protein

At the optical microscopy (OM) level, scrapie-affected sheep showed very intense pathological prion protein (PrPsc) immunoreactivity in lobules VIIb and X (Figure 6). The pattern of deposition was similar. PrPsc immunoreaction was observed in all cerebellar layers, thus revealing a non-homogeneous but constant presence of prion deposition. Small areas of variable size and shape with low immunoreactivity (fine and dispersed granules) were seen close together with other small- or middle-sized areas or “deposits”, with larger diameter granules (confluent in many instances) appearing in far greater numbers (Figure 6).

3. Future Perspectives in the Research

Although many works have focused on natural classical scrapie and experimental scrapie, many issues regarding the pathogenesis and pathogenic course of the disease have not been clarified and need more research. Many cellular and molecular alterations described in the disease are poorly understood or interpreted speculatively, without a certain scientific basis. The involution of the different types of neurons (both dependent on their lineage and/or individually, dependent on their specific status) as well as the neuroglial reactions, which can be neurotoxic as well as neuroprotective, are not sufficiently clear in scrapie. Neurotoxic prion infection and host response “models” are very important research tools for understanding neurodegeneration mechanisms and developing therapeutic strategies, but they necessitate more in-depth study to solve problems and not increase theoretical controversies.

Additional investigations of the morphofunctional alterations of classical scrapie (vacuolization, neurodegeneration, gliosis and abnormal PrP deposits/deposition) are required to fully discover the specific neurotoxic mechanisms of these prion pathologies as well as other generic neurodegeneration mechanisms in brain pathologies.

References

1. Liberski, P. Historical overview of prion diseases: A view from afar. *Folia Neuropathol.* 2012, 50, 1–12.
2. Hadlow, W.J.; Kennedy, R.C.; Race, R.E.; Eklund, C.M. Virologic and neurohistologic findings in dairy goats affected with natural scrapie. *Vet. Pathol.* 1980, 17, 187–199.
3. Vidal, E.; Acín, C.; Foradada, L.; Monzón, M.; Márquez, M.; Monleón, E.; Pumarola, M.; Badiola, J.J.; Bolea, R. Immunohistochemical characterisation of classical scrapie neuropathology in sheep. *J. Comp. Pathol.* 2009, 14, 135–146.
4. Toledano, A.; Alvarez, M.I.; Monleón, E.; Toledano-Díaz, A.; Badiola, J.J.; Monzón, M. Changes induced by natural scrapie in the calretinin-immunopositive cells and fibres of the sheep cerebellar cortex. *Cerebellum* 2012, 11, 593–604.
5. Monzón, M.; Hernández, R.S.; Garcés, M.; Sarasa, R.; Badiola, J.J. Glial alterations in human prion diseases: A correlative study of astroglia, reactive microglia, protein deposition, and neuropathological lesions. *Medicine (Baltimore)* 2018, 97, e0320.
6. Greenlee, J.J. Review: Update on Classical and Atypical Scrapie in Sheep and Goats. *Vet. Pathol.* 2019, 56, 6–16.
7. Imran, M.; Mahmood, S. An overview of human prion diseases. *Viol. J.* 2011, 8, 559.
8. Wood, J.L.; McGill, I.S.; Done, S.H.; Bradley, R. Neuropathology of scrapie: A study of the distribution patterns of brain lesions in 222 cases of natural scrapie in sheep, 1982–1991. *Vet. Rec.* 1997, 140, 167–174.
9. Yang, Q.; Hashizume, Y.; Yoshida, M.; Wang, Y. Neuropathological study of cerebellar degeneration in prion disease. *Neuropathology* 1999, 19, 33–39.

Retrieved from <https://encyclopedia.pub/entry/history/show/22607>